# NEW EVIDENCE FOR PHOTOIONIZATION AS THE DOMINANT EXCITATION MECHANISM IN LINERS

ALEXEI V. FILIPPENKO
Palomar Observatory, California Institute of Technology

## ABSTRACT

Optical spectrophotometry of the nearby QSO MR 2251−178 and the powerful radio sources PKS 1718−649 (a classical Liner) and Pictor A (a type 1 Seyfert galaxy with features of Liners) is presented. MR 2251−178 and Pictor A are undoubtedly photoionized by nonstellar radiation; their spectra exhibit featureless continua, broad Balmer emission (FWZI $\gtrsim$ 20,000 km s$^{-1}$), and prominent forbidden lines spanning a wide range of ionization potentials (e.g., [O I], [Fe VII]). Moreover, both objects are copious emitters of X-rays. Similarly, the strengths of [Ne V] $\lambda$3426 and He II $\lambda$4686 in PKS 1718−649 suggest that gas near the nucleus is photoionized, although the ionizing radiation must be substantially more intense than the nonstellar power law actually observed at optical wavelengths. In all three nuclei, on the other hand, the great strength of [O III] $\lambda$4363 relative to [O III] $\lambda$5007 implies $T_e > 50{,}000$ K, which is incompatible with photoionized low-density clouds ($n_e \approx 10^2$–$10^4$ cm$^{-3}$). Instead, the high temperatures are reminiscent of those in shock-heated gas, and several previous studies concluded that shocks provide the dominant excitation mechanism in both Pictor A and PKS 1718−649.

The dilemma vanishes if relatively dense clouds ($n_e \gtrsim 10^6$–$10^7$ cm$^{-3}$) exist in the narrow-line regions, as has sometimes been suggested for QSOs and type 1 Seyfert galaxies. This paper provides *unambiguous evidence* for such high densities: it is shown that in each object the width of forbidden lines increases with their critical density for collisional deexcitation over the range $10^3 \lesssim n_e(\text{crit}) \lesssim 10^7$ cm$^{-3}$. Dense clouds are optically thick to the Lyman continuum, live close to the nucleus, and move most rapidly.

These data support the contention of Filippenko and Halpern that *a large range in density* among the narrow-line clouds can resolve the [O III] $\lambda$4363 temperature difficulty in photoionization models of Liners. The presence of very similar properties in galactic nuclei having active components of high (MR 2251−178), medium (Pictor A), and low (PKS 1718−649) luminosity suggests that the physical processes in most, if not all, classical AGNs and Liners may be fundamentally the same.

*Subject headings:* galaxies: nuclei — galaxies: Seyfert — quasars — radiation mechanisms — radio sources: galaxies

## I. INTRODUCTION

A large theoretical effort is being made to reproduce the spectral characteristics of active galactic nuclei (AGNs), including Heckman's (1980) "Liners" (low-ionization nuclear emission-line regions). Based on the clear presence of nonstellar ionizing radiation in QSOs and the most luminous Seyfert 1 galaxies, models usually incorporate power-law continua of various strengths to explain the observed intensity ratios of optical emission lines (see Davidson and Netzer 1979, and references therein). Early attempts were moderately successful, but the agreement improved noticeably (Ferland 1981; Ulrich and Péquignot 1980) after the inclusion of rapid charge-exchange reactions (e.g., Butler, Heil, and Dalgarno 1980). Some studies (Ferland and Netzer 1983; Halpern and Steiner 1983) even try to unify all AGNs by varying essentially one parameter, the ratio of ionizing photons to nucleons at the face of a cloud. QSOs and type 1 Seyfert galaxies are characterized by a large "ionization parameter" (U) and exhibit emission lines from highly ionized species, while Liners (which have small U) are defined by $I([\text{O II}]\ \lambda3727) \gtrsim I([\text{O III}]\ \lambda5007)$ and $I([\text{O I}]\ \lambda6300) \gtrsim 0.33 I([\text{O III}]\ \lambda5007)$.

Despite the success of these models, problems exist in the interpretation of Liners. One of the most important is that the observed strengths of transauroral and auroral lines (notably [O III] $\lambda$4363) are sometimes too large compared with the corresponding nebular lines ([O III] $\lambda\lambda$4959, 5007). This led early investigators to ascribe Liner emission to shock heating (Fosbury *et al.* 1978; Heckman 1980; Baldwin, Phillips, and Terlevich 1981), since the observed intensity ratios are a natural consequence of the high temperatures ($\gtrsim 30{,}000$ K) produced by shocks. Another deficiency of photoionization calculations, but generally not of shock models, is that they produce too much He II $\lambda$4686 relative to H$\beta$ (Ferland and Netzer 1983).

Recent studies yield partial solutions to these problems. Keel and Miller (1983) and Rose and Tripicco (1984), for example, show that incomplete removal of the underlying stellar component in the prototypical Liner NGC 1052 has led to serious overestimates of the strength of [O III] $\lambda$4363 (Koski and Osterbrock 1976; Fosbury *et al.* 1978). The new, smaller values imply lower $T_e$ and eliminate some of the conflict with simple photoionization models. Moreover, Péquignot (1984) postulates that much of the *ionizing* continuum in NGC 1052 has the shape of a hot ($T \approx 8 \times 10^4$ K) blackbody rather than a power law, resulting in relatively weak He II $\lambda$4686.

The bright galaxy NGC 7213 (Filippenko and Halpern 1984, hereafter FH; Halpern and Filippenko 1984) provides additional clues. Gas near its nucleus is clearly photoionized by nonstellar radiation, and yet the optical spectrum also exhibits many "shock" characteristics of Liners (including strong

[O III] $\lambda 4363$). An observed correlation between the width of forbidden lines and their critical densities for deexcitation, however, reveals a *wide range of densities* ($n_e \approx 10^3$–$10^7$ cm$^{-3}$) among clouds in the narrow-line region (NLR). This information is subsequently used to show that the "shock" features can be understood entirely in the context of photoionization models, and it is suggested that similar conditions prevail in classical Liners.

One is tempted to speculate that at least some nearby galaxies harbor a massive black hole which is running out of "fuel" (Gunn 1979). The analysis of NGC 7213 suggests that these are Liners, since the dominant physical processes within them may be fundamentally the same as in QSOs. Of course, a large number of objects must be investigated before drawing definitive conclusions, but this paper presents observations which strongly support the above arguments. Density stratification in the NLR is evident in PKS 1718−649 (a classical Liner), Pictor A (a Seyfert 1 galaxy with features of Liners), and MR 2251−178 (a nearby QSO), demonstrating that the physical conditions in objects spanning a wide range in the ratio of nuclear (unresolved) to disk (resolved) luminosity can be comparable to those in NGC 7213.

## II. OBSERVATIONS

Data were obtained in 1983 August with the Boller & Chivens Cassegrain spectrograph on the 2.5 m du Pont reflector at Las Campanas Observatory. A journal of observations is given in Table 1. Shectman's (1981) new Intensified Reticon detector, an improved version of the original instrument (Shectman and Hiltner 1976), was used. Bausch and Lomb gratings with 600 and 1200 grooves mm$^{-1}$ provided typical resolutions (in first order) of roughly 5 Å and 2.5 Å, respectively. The wavelength scale was determined by fitting a fifth-order polynomial to the positions of unblended emission lines in comparison spectra (Fe, Ar, Ne) obtained before and after each observation.

To minimize light losses caused by atmospheric dispersion (Filippenko 1982), the long dimension of the rectangular ($2'' \times 4''$) entrance aperture was aligned along the parallactic angle corresponding to the midpoint of each observation. The relatively large separation between the "object" and "sky" apertures ($27''.4$) ensured that light from the outer portions of the galaxies did not contribute significantly to the sky measurements. Coincidence losses were negligible due to the faintness of all objects, except in the [O III] $\lambda 5007$ line of MR 2251−178 (§ V$a$). Calibration of the spectrograph's response as a function of wavelength was achieved with faint, relatively

featureless standard stars (Filippenko and Greenstein 1984). Local variations in the sensitivity of the detector were removed with lengthy exposures of the featureless continuum from a hot tungsten lamp. Stability of these "flat fields" from one night to the next was excellent ($\sim 1\%$–$2\%$).

Constraints imposed by other projects limited observations to only one grating angle per object for the low-resolution data. No filters were used so that the entire optical spectrum could be measured; consequently, second-order contamination longward of $\sim \lambda 6200$ is present. This is generally not serious because most galaxies are much fainter at blue and ultraviolet (UV) wavelengths than in the red. The standard stars, however, are somewhat bluer than the light of galactic bulges, resulting in greater second-order contamination and hence an overestimate of the spectrograph's red sensitivity. Since it was not possible to precisely calibrate this effect, the corrected emission-line intensities of Pictor A and PKS 1718−649 are uncertain by $\pm 10\%$–$15\%$ longward of $\sim \lambda 6200$.

## III. PKS 1718−649

PKS 1718−649 is a D galaxy ($m_v \approx 15.5$) at a distance of $\sim 85$ Mpc.[1] It exhibits a powerful, inverted radio spectrum from 408 to 2700 MHz and strong optical emission lines (Savage 1976; Fosbury *et al.* 1979, hereafter FMGV). Faint spiral arms surrounding the bright bulge are visible in deep photographs, and H I accounts for fully 6% of the object's total mass. Using a $3'' \times 6''$ aperture, FMGV found that $I([O\ II]\ \lambda 3727)/I([O\ III]\ \lambda 5007) \approx 1.3$ and $I([O\ I]\ \lambda 6300)/I([O\ III]\ \lambda 5007) \approx 1.5$; PKS 1718−649 is therefore clearly a Liner (Heckman 1980). Its spectral similarity to NGC 1052, together with the absence of a blue nonstellar excess, led them to conclude that the emission lines are produced by shock-heated gas.

FMGV noticed that [O I] $\lambda 6300$ is both significantly broader than other emission lines and over a factor of 3 stronger than [O I] $\lambda 6364$. They decided that it is blended with [S III] $\lambda 6312$, but this is unlikely considering the weakness of [S III] in classical Seyfert galaxies. A more plausible conclusion is that the [O I] lines are intrinsically broad, and that [O I] $\lambda 6364$ appears too weak due to underlying Fe I $\lambda\lambda 6355$, 6359 absorption (Filippenko and Sargent 1985). The resemblance to NGC 7213 (FH) suggests that PKS 1718−649 may provide important clues to the Liner phenomenon, so high-quality spectra of its nucleus were obtained.

---

[1] Unless otherwise noted, a Hubble constant of 50 km s$^{-1}$ Mpc$^{-1}$ is assumed.

TABLE 1

JOURNAL OF OBSERVATIONS

| Object | Date (UT) | Time (s) | Grooves mm$^{-1}$ [a] | Aperture (arcsec) | $R$(Å)[b] | $\Delta\lambda$ (Å) | Standard Star | Air Mass (begin/end) | PA (deg) | See[c] |
|---|---|---|---|---|---|---|---|---|---|---|
| PKS 1718−649 ....... | 1983 Aug 9 | 3600 | 600 | $2 \times 4$ | 4–5 | 3490–7170 | G158−100 | 1.24/1.25 | 180 | 1 |
|  | 1983 Aug 14 | 3000 | 1200 | $2 \times 4$ | 2–3 | 3210–5100 | G158−100 | 1.24/1.24 | 180 | 1 |
| Pictor A ............... | 1983 Aug 11 | 4200[d] | 600 | $2 \times 4$ | 4–5 | 3890–7580 | G24−9 | 1.49/1.22 | 90 | 1.5 |
| MR 2251−178 ........ | 1983 Aug 14 | 1200 | 1200 | $8 \times 8$ | 5–6 | 3210–5100 | G158−100 | 1.09/1.06 | 90 | 1 |
|  | 1983 Aug 14 | 1200 | 1200 | $8 \times 8$ | 5–6 | 4730–6100 | G158−100 | 1.06/1.04 | 90 | 1 |
| IC 4889 ............... | 1983 Aug 13 | 2800[d] | 600 | $2 \times 4$ | 4–5 | 3900–7580 | G24−9 | 1.18/1.13 | 136 | 1.5 |
|  | 1983 Aug 14 | 2400 | 1200 | $2 \times 4$ | 2–3 | 3210–5100 | G158−100 | 1.12/1.11 | 165 | 1 |

[a] Number of grooves mm$^{-1}$ for each of the two gratings, blazed at $\sim \lambda 5000$.
[b] Resolution ($R$) denotes FWHM of unblended emission lines.
[c] Very approximate FWHM of seeing disk, in arc seconds.
[d] Cirrus clouds were present during the integration.

### a) Stellar and Nonstellar Continua

In overall appearance the new data resemble those of FMGV. Close inspection of the spectrum, however, reveals a faint blue excess which cannot be produced by the old stellar population. To quantify it, the continuum was decomposed into the spectrum of a giant elliptical galaxy (Yee and Oke 1978) and a power law ($f_v \propto v^{-\alpha}$), as described by Halpern and Filippenko (1984). Ignoring regions contaminated by emission lines, least squares fits were performed to obtain the reddening and the ratio of nonstellar to total flux at $\lambda 5460$. An accurate determination of the spectral index was impossible due to the dominance of starlight and the small wavelength range, but $\alpha = 1.5 \pm 1.1$ produced good results. This is fairly representative of QSOs and Seyfert galaxies (Koski 1978; Malkan and Sargent 1982; Malkan and Filippenko 1983).

The decomposition is shown in Figure 1a. A faint nonstellar component contributes only $\sim 6\%$ of the observed flux at $\lambda 5460$. Its relative prominence increases at shorter wavelengths, and near $\lambda 3200$ it is roughly half the strength of starlight. Dilution of the Ca II K ($\lambda 3934$) and H ($\lambda 3968$) absorption lines is calculated to be small ($\sim 13\%-14\%$). These results are sensitive to the range of wavelengths and value of $\alpha$ used in the decomposition, but qualitatively the conclusions remain unchanged.

Using the usual curve of Whitford (1958), the derived reddening corresponds to $A_v = 3.2E_{B-V} = 0.70$ mag. This is larger than the expected Galactic value of $\sim 0.3$ mag (Burstein and Heiles 1982). Dust in the nuclear region (FMGV) can probably account for the excess reddening.

### b) Emission Lines

Old stars dominate the spectrum and affect measurements of emission lines, producing unacceptable inaccuracies in crucial diagnostics such as [O III] $\lambda 4363$ and He II $\lambda 4686$. The starlight was therefore removed with a template devoid of emission. As in NGC 7213, the S0 galaxy IC 4889 was a particularly suitable choice because the metallicity and stellar velocity dispersion in its nucleus are similar to those of PKS 1718−649.

FH describe the procedure in detail. First, the nonstellar component was subtracted from the dereddened spectrum of PKS 1718−649 (Fig. 2a). The overall spectral shape of IC 4889 was then adjusted to match that of the object (thereby artificially removing differences in reddening, etc.), and its metallicity was decreased slightly. Finally, weak [O II] $\lambda 3727$ was excised, resulting in the spectrum shown in Figure 2b. Subtraction of the template from the object produced the net emission-line spectrum (Fig. 2c). Regions blueward of $\lambda 3600$ and
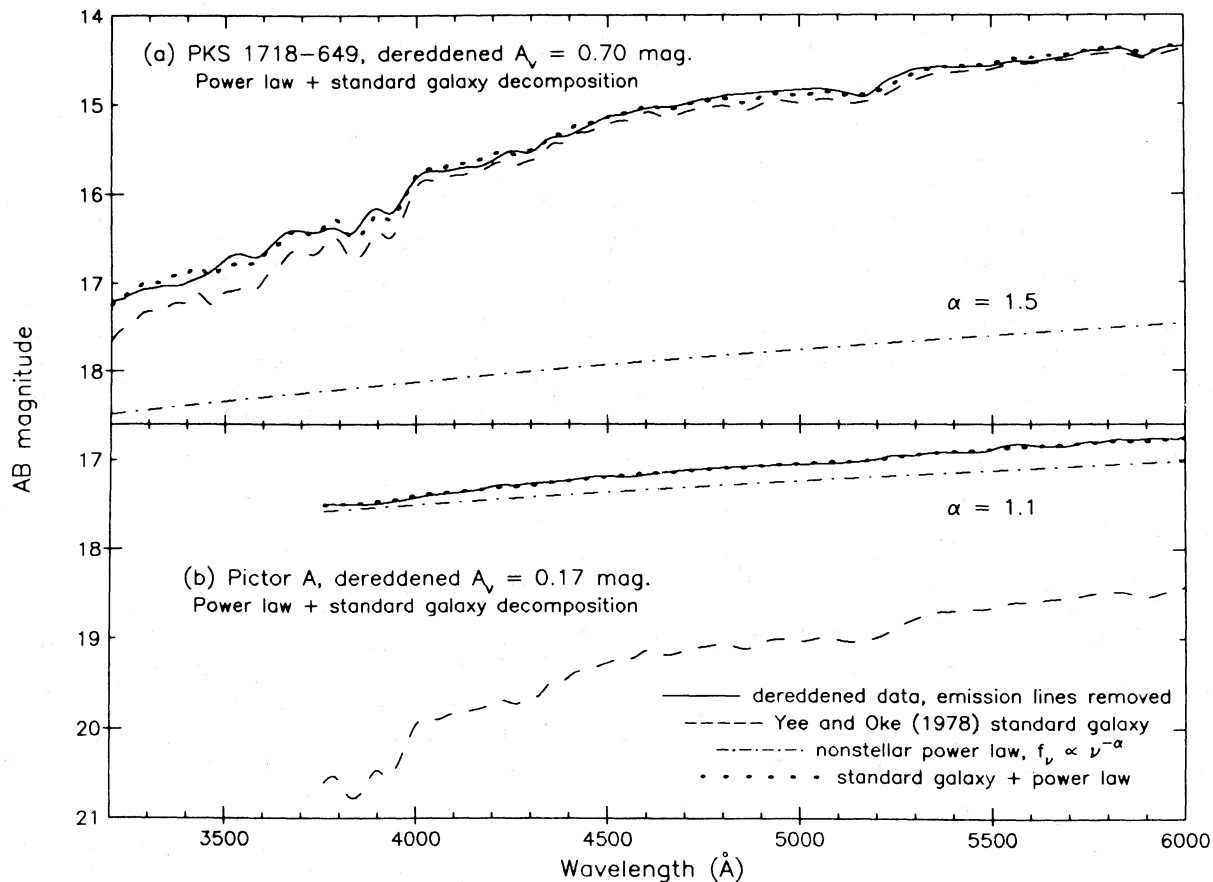


FIG. 1.—The smoothed continua of (a) PKS 1718−649 and (b) Pictor A are decomposed into an old stellar population and a nonstellar power law of index $\alpha$. Magnitude AB $= -2.5$ Log ($f_v$) $- 48.6$, where $f_v$ is in ergs s$^{-1}$ cm$^{-2}$ Hz$^{-1}$. The absolute flux calibrations are uncertain. Least squares fits were used to derive the reddening of the continuum, the contribution of stars at $\lambda 5460$, and the approximate value of $\alpha$. At optical wavelengths, PKS 1718−649 consists mostly of starlight, whereas Pictor A is dominated by nonstellar radiation.
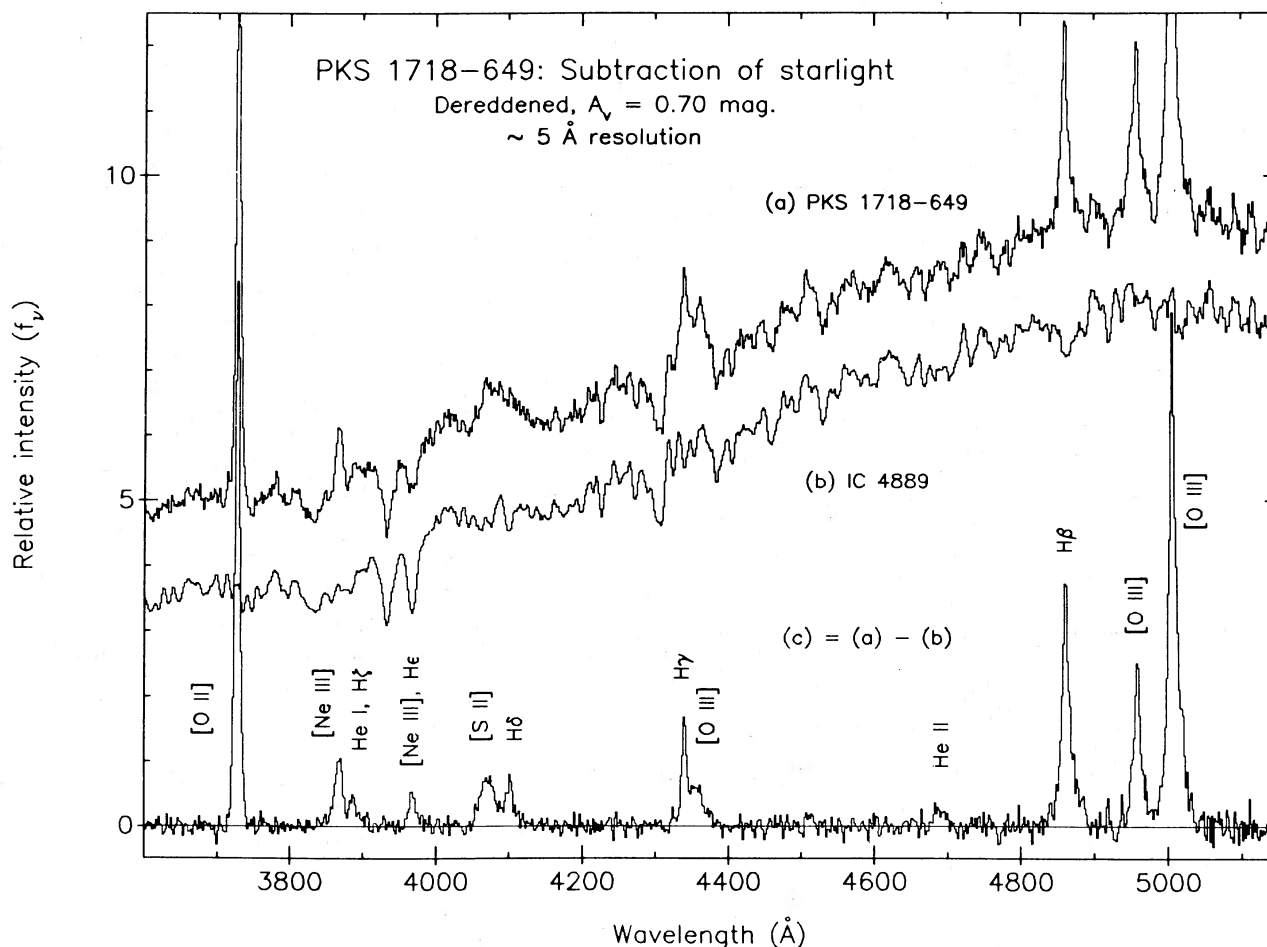
FIG. 2.—Spectra of (a) PKS 1718 − 649, (b) the template galaxy IC 4889, and (c) the emission-line component of PKS 1718 − 649 are shown on the same ordinate scale but with different zero-point offsets. The nonstellar continuum (Fig. 1a) was removed in (a), and the spectrum dereddened by $A_v = 3.2E_{B-V} = 0.70$ mag. Small adjustments were made to the metallicity and overall shape of IC 4889 to make them match those of PKS 1718 − 649. Note the faint emission lines (such as He II $\lambda$4686) in (c) which were previously hidden among absorption lines.

redward of $\lambda$5150 were excluded because of poor signal-to-noise ($S/N$) ratios in either PKS 1718 − 649 or IC 4889.

Benefits of the subtraction are obvious. The [Ne III] $\lambda$3967 + He blend, previously hidden in Ca II H absorption, is present. Similarly, the [S II] $\lambda$4069 + H$\delta$ and [O III] $\lambda$4363 + H$\gamma$ composites are much easier to analyze. [O III] $\lambda$4363 can be measured with greater accuracy since the prominent "high point" in the underlying stellar continuum has been properly removed. Even He II $\lambda$4686, which was not suspected in the original spectrum (Fig. 2a), is visible.

Emission lines in Figure 2c have different widths, and in several cases (e.g., [O III] $\lambda$5007, H$\beta$) strong wings make the profiles appear distinctly non-Gaussian. These results are confirmed by the data in the vicinity of H$\alpha$ (Fig. 3a). [O I] $\lambda$6300 is as broad as the combined [S II] $\lambda\lambda$6716 + 6731 doublet, and its profile exhibits wings of greater prominence than a Gaussian having the same full width at half-maximum (FWHM).

An even broader component is apparent in the H$\alpha$ + [N II] blend, especially on the red side. It is almost certainly produced by H$\alpha$ rather than [N II], since the adjacent [S II] lines (which are formed under roughly the same physical conditions as [N II]) do not have extended wings. A full width at zero-intensity (FWZI) of $\sim$4500 Å makes it qualitatively similar to (but less intense and narrower than) that in classical type 1

Seyferts. Together with the weak nonstellar continuum, the inconspicuous broad-line region (BLR) suggests that PKS 1718 − 649 may have one of the least luminous Seyfert 1 nuclei discovered to date. Spectra of many other Liners also contain very faint, broad H$\alpha$ emission (Filippenko and Sargent 1985).

To facilitate quantitative analysis of the data, the intensity, FWHM, full width at 10% intensity (FW10), and equivalent width (EW) of each emission line were carefully measured. The traditional FWZI was generally not chosen because it is difficult to determine and is very dependent on the $S/N$ ratio. All intensity measurements are listed in Table 2. Typical errors are generally $\lesssim$10% for strong, unblended lines, 15%–20% for blends or weaker lines, and up to $\sim$100% for the faintest features (denoted by a colon). These values do not include possible inaccuracies in the overall calibration of the spectrum. Widths are given in Table 3.

In a few cases special procedures were used to deblend lines. The assumed strength and width of [N II] $\lambda$6583 were varied to yield a smooth H$\alpha$ profile. Comparison of H$\alpha$ and H$\beta$ showed excellent agreement except in the wings of the broad component, which is virtually absent in the latter line. By appropriately scaling the H$\beta$ profile, it was possible to isolate [O III] $\lambda$4363 from the blend with H$\gamma$. H$\delta$ was subtracted from [S II] $\lambda\lambda$4069 + 4076 in a similar manner.
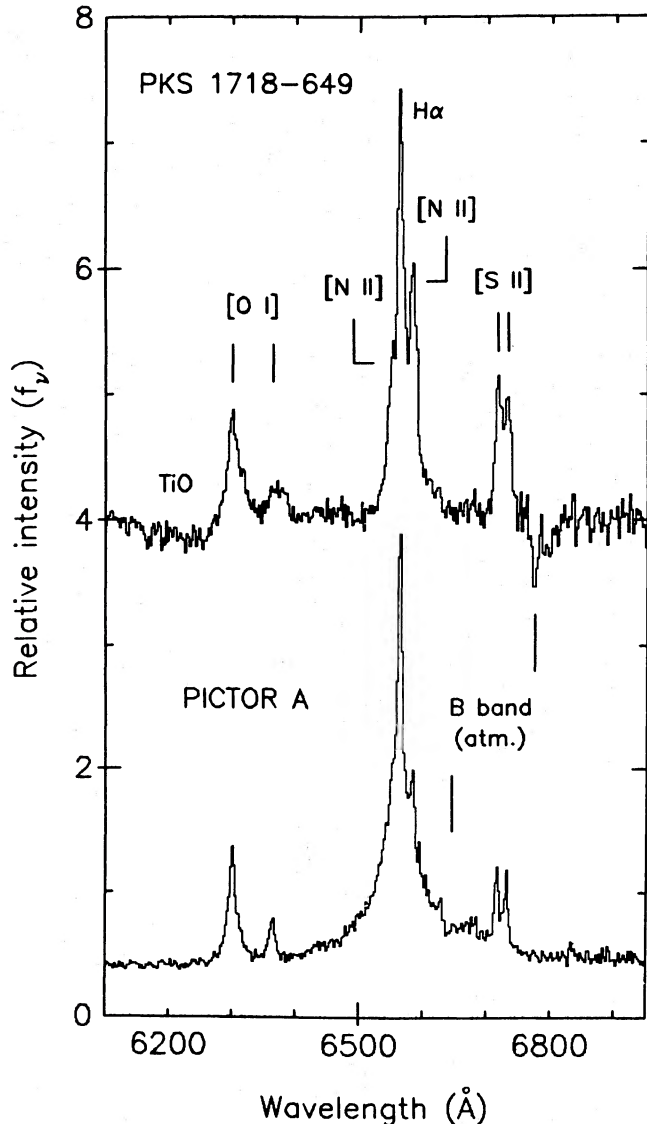
PHOTOIONIZATION IN LINERS



FIG. 3.—Spectra of PKS 1718−649 and Pictor A demonstrate the presence of broad Hα emission and the markedly different profiles of [O I] and [S II]. Stellar and atmospheric absorption were not removed. Balmer lines have prominent, roughly logarithmic wings in Pictor A.

The largest discrepancy between the new intensity ratios and those measured by FMGV occurs in $I([N \text{ II}]\ \lambda\lambda6548 + 6583)/I(H\alpha)$. Since FMGV used three Gaussians of equal width to decompose the blend in their relatively low-resolution data ($\sim 10$ Å), too much of the Hα flux was attributed to [N II]. Many other differences, including FMGV's nondetection of weak emission such as He II $\lambda4686$, can be explained by contamination from underlying absorption lines. Note that their absolute flux of Hβ is a factor of $\sim 2.8$ larger than that quoted here, but the entrance apertures are different and neither study claims photometric accuracy.

Table 2 indicates the presence of [Ne v ] $\lambda3426$. Since appreciable [Ne v] is not produced by low-velocity shocks (100–150 km s$^{-1}$) or in normal H II regions around OB stars, it is highly likely that *gas is photoionized by the nonstellar continuum* described in § IIIa. The detection of He II $\lambda4686$ supports this conclusion. Although an extrapolation of the derived power

law past the Lyman limit fails by nearly a factor of 10 to produce the dereddened Hα flux of $2.0 \times 10^{-13}$ ergs s$^{-1}$ cm$^{-2}$, such a calculation is probably oversimplified; most bright QSOs and type 1 Seyferts have much more radiation at UV wavelengths than expected from a comparison with the optical power law (e.g., Malkan and Sargent 1982; Oke, Shields, and Korycansky 1984). *If* such an excess also exists in PKS 1718−649, it may account for the observed flux of Hα (see also Péquignot 1984).

After correcting for extinction ($A_v = 0.70$ mag), the luminosity of the power law at $\lambda4800$ is $\sim 2.4 \times 10^{27}$ ergs s$^{-1}$ Hz$^{-1}$, while that of Hα emission is $1.8 \times 10^{41}$ ergs s$^{-1}$. Transforming from $H_0 = 50$ km s$^{-1}$ Mpc$^{-1}$ to $H_0 = 75$, these values place PKS 1718−649 among low-luminosity type 2 Seyferts in Figure 2 of Shuder (1981). PKS 1718−649 was not detected in the X-ray survey of Piccinotti *et al.* (1982, completeness limit $\sim 3.1 \times 10^{-11}$ ergs s$^{-1}$ cm$^{-2}$), but this is not surprising since the expected X-ray flux (2–10 keV) is only $\sim 8 \times 10^{-12}$ ergs s$^{-1}$ cm$^{-2}$ if a mean $L_x(2$–$10$ keV$)/L(H\alpha)$ ratio of $\sim 40$ for AGNs is adopted (Elvis, Soltan, and Keel 1984). The data of Halpern and Steiner (1983), which yield $L_x(0.5$–$4.5$ keV$)/L(H\alpha) \approx 20$ for Liners, together with the fact that soft X-rays (0.5–4.5 keV) are systematically absorbed by gas and dust in low-luminosity AGNs (Lawrence and Elvis 1982), support the value of 40 used above.[2]

### c) Evidence for High Densities

The ratio $R \equiv I([O \text{ III}]\ \lambda\lambda4959 + 5007)/I([O \text{ III}]\ \lambda4363)$ is $\sim 12$ in PKS 1718−649. This is remarkably small and implies that $T_e \approx 8 \times 10^4$ K if $n_e \approx 10^4$ cm$^{-3}$. $T_e$ becomes still larger if a density of $\sim 250$ cm$^{-3}$, obtained from the observed ratio $I([S \text{ II}]\ \lambda6716)/I([S \text{ II}]\ \lambda6731) \approx 1.16$, is adopted. Even if the data are not dereddened, the derived value of $T_e$ is very high ($> 6 \times 10^4$ K). Such temperatures are incompatible with photoionization models, which always predict $T_e \lesssim 20,000$ K for the $O^{++}$ region, but they may be prevalent in shock-heated gas.

A reconciliation with photoionization can be made if one does not assume that the density in the $O^{++}$ zone is low. At high $n_e$ ($\sim 10^6$–$10^7$ cm$^{-3}$), collisional deexcitation of the [O III] $\lambda\lambda4959$, 5007 lines is greater relative to that of [O III] $\lambda4363$ because the former are associated with a smaller critical density than the latter; $R$ therefore shifts to small values even at low temperatures. If $\text{Log } n_e \equiv \log_{10} n_e \approx 6.5$ is representative of the $O^{++}$ zone in PKS 1718−649, for example, the ratio $R \approx 12$ indicates $T_e \approx 11,000$ K.

Although Ferland and Netzer (1983) considered high densities improbable in Liners, FH provide undeniable evidence for them in the Liner/Seyfert galaxy NGC 7213: there is an excellent correlation between width and $n_e$(crit) for 16 forbidden lines. Even lines emitted by the *same* species (such as [O II] $\lambda\lambda3726$, 3729 and [O II] $\lambda\lambda7319$, 7330) maintain the correlation by exhibiting different widths. Since line emission per unit mass rises linearly with $n_e$ below $n_e$(crit) and remains constant above it, different forbidden lines act as effective tracers of $n_e$ in the NLR of NGC 7213, which clearly has a wide range of densities among its clouds. Evidence for a variety of densities would not have been as compelling (in the absence of other information) if width were better correlated with ionization potential ($\chi$) than with critical density (Filippenko 1985).

TABLE 2

EQUIVALENT WIDTHS AND RELATIVE INTENSITIES OF EMISSION LINES[a]

| LINE | PKS 1718−649 | | | PICTOR A | | MR 2251−178 | |
|---|---|---|---|---|---|---|---|
| | EW (Å) | $F/F(N2)$ | $I/I(N2)$[b] | EW (Å) | $F/F(N2)$ | EW (Å) | $F/F(N2)$ |
| [Ne v] $\lambda3346$ | 4.: | 0.04: | 0.06: | — | — | 1.: | 0.03: |
| [Ne v] $\lambda3426$ | 10. | 0.12 | 0.16 | — | — | 4.9 | 0.12 |
| [O II] $\lambda3727$ | 57. | 0.91 | 1.18 | — | — | 8.7 | 0.18 |
| H I $\lambda3798$ | ... | ... | ... | — | — | 0.2: | 0.004: |
| H I $\lambda3835$ | ... | ... | ... | 3.: | 0.03: | 0.5: | 0.01: |
| [Ne III] $\lambda3869$ | 10. | 0.19 | 0.24 | 22. | 0.21 | 9.0 | 0.16 |
| He I + H8 $\lambda3889$ | 3.6 | 0.070 | 0.087 | 8.2 | 0.080 | 2.8 | 0.050 |
| [Ne III] + Hε $\lambda3970$ | 4.1 | 0.090 | 0.11 | 14. | 0.14 | 6.0 | 0.091 |
| [S II] $\lambda4071$ | 8.4 | 0.21 | 0.25 | 9.9 | 0.096 | 0.7: | 0.01: |
| Hδ $\lambda4102$ | 4.7 | 0.12 | 0.14 | 18. | 0.17 | 10. | 0.14 |
| [Fe II] $\lambda4250$?[c] | ... | ... | ... | ... | ... | 0.3: | 0.004: |
| [Fe II] $\lambda4281$?[c] | ... | ... | ... | ... | ... | 0.6: | 0.008: |
| Hγ $\lambda4340$ | 6.8 | 0.22 | 0.25 | 37. | 0.35 | 33. | 0.40 |
| [O III] $\lambda4363$ | 2.7 | 0.096 | 0.11 | 9.7 | 0.096 | 11. | 0.13 |
| He I $\lambda4471$ | ... | ... | ... | ... | ... | 0.4: | 0.004: |
| He II $\lambda4686$ | 1.1 | 0.048 | 0.05 | 15. | 0.14 | 2.1[d] | 0.02[d] |
| Hβ $\lambda4861$ | 11. | 0.52 | 0.53 | 93. | 0.85 | 150.[e] | 1.55[e] |
| [O III] $\lambda4959$ | 6.2 | 0.31 | 0.31 | 39. | 0.35 | 33. | 0.34 |
| [O III] $\lambda5007$ | 20. | 1.00 | 1.00 | 110. | 1.00 | 98.[f] | 1.00[f] |
| [Fe VII] $\lambda5159$ | ... | ... | ... | 3.: | 0.03: | 2.: | 0.02: |
| [N I] $\lambda5200$ | 0.2: | 0.01: | 0.01: | 2.: | 0.02: | 1.: | 0.01: |
| Fe II $\sim\lambda5270$?[g] | ... | ... | ... | 5.: | 0.05: | ... | ... |
| [O I] $\lambda5577$ | ... | ... | ... | 2.: | 0.02: | ... | ... |
| [Fe VII] $\lambda5721$ | ... | ... | ... | 2.: | 0.02: | — | — |
| He I $\lambda5876$ | 0.7: | 0.04: | 0.04: | 7.9 | 0.068 | — | — |
| [O I] $\lambda6300$* | 18. | 1.10 | 0.90 | 57. | 0.48 | — | — |
| [O I] $\lambda6364$* | 6.2 | 0.37 | 0.30 | 16. | 0.14 | — | — |
| [N II] $\lambda6548$* | 3.1 | 0.19 | 0.15 | 4.0 | 0.033 | — | — |
| Hα $\lambda6563$* | 40.7 | 2.44 | 1.93 | 515. | 4.28 | — | — |
| [N II] $\lambda6583$* | 9.3 | 0.56 | 0.44 | 12. | 0.10 | — | — |
| [S II] $\lambda6716$* | 7.6 | 0.45 | 0.35 | 15. | 0.12 | — | — |
| [S II] $\lambda6731$* | 6.6 | 0.39 | 0.30 | 15. | 0.12 | — | — |
| $A_v$ (mag)[h] | 0.70 | | | 0.17 | | 0.05 | |
| $F(N2)$ (ergs s$^{-1}$ cm$^{-2}$)[i] | $5.0 \times 10^{-14}$ | | | $5.9 \times 10^{-14}$ | | $5.6 \times 10^{-13}$ | |
| $I(N2)$ (ergs s$^{-1}$ cm$^{-2}$)[j] | $1.1 \times 10^{-13}$ | | | $7.1 \times 10^{-14}$ | | $5.9 \times 10^{-13}$ | |

[a] Dash (—): line not available in data. Dots (...): extremely weak or nonexistent line. Colon (:): very uncertain measurement ($\pm 100\%$). Asterisk (*): flux calibration affected by second-order contamination ($\pm 10\%$–$15\%$).

[b] $A_v = 3.2E_{B-V} = 0.70$ mag used to deredden the observed fluxes, $F$. Reddening in Pictor A and MR 2251−178 is small, so $I(\lambda) \approx F(\lambda)$.

[c] Lines identified by Bergeron et al. 1983.

[d] Includes only the well-defined narrow component.

[e] Contaminated to some extent by the broad component of He II $\lambda4686$.

[f] Data affected by coincidence losses. Intensity replaced by 2.96 times $F([O III]\ \lambda4959)$.

[g] Possibly Fe II emission, but it is absent elsewhere in the spectrum of Pictor A.

[h] Derived from continuum decomposition of PKS 1718−649 and Pictor A. Galactic extinction for MR 2251−178.

[i] N2 ≡ [O III] $\lambda5007$. Absolute flux accurate only in MR 2251−178. Extinction not removed.

[j] Same as preceding note, but with extinction corresponding to the given value of $A_v$ removed.

The same arguments are directly applicable to PKS 1718−649. Figure 4a illustrates the dependence of FW10 on $\chi$ for 13 different forbidden lines.[3] Estimates of the errors are shown along with the measured widths. A correlation may be present, but the scatter is large. The ionization level of clouds therefore cannot be described by a single parameter which changes monotonically with decreasing distance from the photoionizing source, unlike the case if all the gas were optically thin and of uniform density. If $\chi$ is replaced with $n_e$(crit), on the other hand (Fig. 4b), the correlation coefficient

rises from 0.28 to 0.91, and a correlation is certain. As summarized in Table 4, similar results are obtained for the FWHM of lines.

An important point is that lines from the *same species* and characterized by *different* values of $n_e$(crit), such as the blue and red [S II] doublets as well as [O III] $\lambda\lambda4959$, 5007 and [O III] $\lambda4363$, greatly *strengthen* the correlation between width and $n_e$(crit). Pelat, Alloin, and Fosbury (1981), who analyzed the type 1 Seyfert NGC 3783, also suggested that line width increases with $n_e$(crit), but their correlation between width and $\chi$ was equally good because they had no lines that were capable of *unambiguously* discriminating between $\chi$ and $n_e$(crit).

A particularly significant line in PKS 1718−649 is [O I] $\lambda6300$ [$n_e$(crit) $\approx 1.4 \times 10^6$ cm$^{-3}$], whose large strength and width relative to [S II] $\lambda\lambda6716$, 6731 [$n_e$(crit) $\approx 2 \times 10^3$ cm$^{-3}$] indicate that the high-velocity clouds must be both dense and

[3] The ionization potential used here and by FH corresponds to the actual ion under consideration, rather than to the next less-ionized species like in some studies (e.g., Pelat, Alloin, and Fosbury 1981; De Robertis and Osterbrock 1984). Also, the critical densities were calculated with assumed temperatures ranging from 10,000 K (for low-ionization lines) to 20,000 K (for [Ne v]).

TABLE 3

WIDTHS OF FORBIDDEN LINES (km s$^{-1}$)[a]

| LINE[b] | $n_e$(crit) (cm$^{-3}$) | $\chi$ (eV)[c] | PKS 1718−649 | | PICTOR A | | MR 2251−178 | |
|---|---|---|---|---|---|---|---|---|
| | | | FWHM | FW10 | FWHM | FW10 | FWHM | FWZI |
| [S II] $\lambda6716$ ............ | $1.2 \times 10^3$ | 23.3 | 500 | 1000 | 300 | 650 | ... | ... |
| [N I] $\lambda5199$[d] ............ | $1.3 \times 10^3$ | 14.5 | ... | ... | 250 | 400 | ... | ... |
| [O II] $\lambda3727$[d] ......... | $3.0 \times 10^3$ | 35.1 | 450 | 820 | ... | ... | 200 | 700 |
| [S II] $\lambda6731$ ............ | $3.1 \times 10^3$ | 23.3 | 500 | 990 | 340 | 720 | ... | ... |
| [N II] $\lambda6583$ ........... | $9.2 \times 10^4$ | 29.6 | 500 | 1000 | 320 | 690 | ... | ... |
| [O III] $\lambda4959$ ......... | $7.9 \times 10^5$ | 54.9 | 550 | 1700 | 470 | 2020 | 390 | 2980 |
| [O III] $\lambda5007$ ......... | $7.9 \times 10^5$ | 54.9 | 570 | 1950 | 480 | 1820 | 410 | 3000 |
| [O I] $\lambda6300$ ........... | $1.4 \times 10^6$ | 13.6 | 1200 | 2450 | 600 | 2210 | ... | ... |
| [O I] $\lambda6364$ ........... | $1.4 \times 10^6$ | 13.6 | 1250 | 2200 | 580 | 1870 | ... | ... |
| [S II] $\lambda4069$ ........... | $1.7 \times 10^6$ | 23.3 | 1390 | 2800 | 690 | 2200 | ... | ... |
| [Ne III] $\lambda3869$ ........ | $1.2 \times 10^7$ | 63.5 | 950 | 2450 | 650 | 2170 | 510 | 3600 |
| [Ne III] $\lambda3967$ ........ | $1.2 \times 10^7$ | 63.5 | 900 | 1850 | 540 | 1850 | 570 | 3300 |
| [Ne V] $\lambda3346$ ......... | $1.9 \times 10^7$ | 126.2 | 1750 | ... | ... | ... | 450 | 2700 |
| [Ne V] $\lambda3426$ ......... | $1.9 \times 10^7$ | 126.2 | 2050 | 3100 | ... | ... | 640 | 4000 |
| [O III] $\lambda4363$ ......... | $3.0 \times 10^7$ | 54.9 | 1300 | 2900 | 1000 | 2600 | 800 | 3850 |

[a] FWHM = full width at half-maximum; FW10 = full width at 10% intensity; FWZI = full width at zero intensity. Resolution of spectrograph removed.

[b] Listed in order of increasing critical density.

[c] Ionization potential of species producing the emission line.

[d] Widths refer to each of the two blended components.

*optically thick.* Of course, Seyfert galaxies having a good correlation between line width and ionization potential $\chi$ (e.g., De Robertis and Osterbrock 1984), but in which [O I] $\lambda6300$ is the *only* measured line that can possibly discriminate between $\chi$ and $n_e$(crit), do not yield definitive conclusions concerning the presence or absence of high-density gas. Dense clouds can still exist near the nucleus, but no broad [O I] $\lambda6300$ is emitted if they are optically *thin* since most of the oxygen is at least singly ionized.

Thus, clouds of high density ($10^6$–$10^7$ cm$^{-3}$) clearly play a major role in determining the emission-line spectrum of PKS 1718−649. These densities are a factor of ~10 larger than even the highest ones normally found in the NLR of Seyfert galaxies and adopted in photoionization models (e.g., Oke 1978). Exceptions to this are several broad-line radio galaxies (Osterbrock, Koski, and Phillips 1976), Seyfert 1 galaxies (Neugebauer *et al.* 1976; Osterbrock 1977), and quasars (e.g.,

Baldwin 1975), in which high densities had been proposed to alleviate the problem of high [O III] temperatures. As discussed in detail by FH, regions of high density enhance auroral and transauroral lines (e.g., [O III] $\lambda4363$, [S II] $\lambda4069$) relative to the nebular emission and mimic the effects of high $T_e$. No conflicts exist with the temperatures required by photoionization models. The simultaneous presence of low densities (derived from the [S II] doublet) precludes the use of simple, single-density models.

Several other properties of the emission lines should be mentioned. [O III] $\lambda4959$ and [O III] $\lambda5007$ are blueshifted by 40–50 km s$^{-1}$ with respect to low-ionization lines, which share the systemic (absorption-line) velocity of ~4290 km s$^{-1}$. This can easily be explained in models which incorporate dust in the narrow-line clouds (FH). Not much dust is necessary to produce such a small difference, and very little intrinsic reddening of the emission lines in the NLR is indicated by the

TABLE 4

UNWEIGHTED LINE WIDTH CORRELATIONS: $y = A + Bx$

| Object | Relation[a] | N[b] | A | B | $\sigma_A$ | $\sigma_B$ | $r$[c] | Probability[d] |
|---|---|---|---|---|---|---|---|---|
| PKS 1718−649 ....... | FWHM vs. $n_e$(crit) | 13[e] | 2.27 | 0.113 | 0.16 | 0.027 | 0.78 | 0.998 |
| | FWHM vs. $\chi$ | 13[e] | 2.71 | 0.131 | 0.36 | 0.227 | 0.17 | 0.424 |
| | FW10 vs. $n_e$(crit) | 13 | 2.55 | 0.122 | 0.10 | 0.017 | 0.91 | ~1.000 |
| | FW10 vs. $\chi$ | 13 | 2.94 | 0.200 | 0.32 | 0.205 | 0.28 | 0.651 |
| Pictor A .............. | FWHM vs. $n_e$(crit) | 12 | 2.11 | 0.103 | 0.09 | 0.015 | 0.91 | ~1.000 |
| | FWHM vs. $\chi$ | 12 | 2.32 | 0.242 | 0.29 | 0.192 | 0.37 | 0.764 |
| | FW10 vs. $n_e$(crit) | 12 | 2.23 | 0.161 | 0.13 | 0.022 | 0.92 | ~1.000 |
| | FW10 vs. $\chi$ | 12 | 2.47 | 0.448 | 0.44 | 0.294 | 0.43 | 0.841 |
| MR 2251−178 ........ | FWHM vs. $n_e$(crit) | 8 | 1.86 | 0.125 | 0.13 | 0.019 | 0.94 | 0.999 |
| | FWHM vs. $\chi$ | 8 | 1.77 | 0.493 | 0.61 | 0.331 | 0.52 | 0.813 |
| | FWZI vs. $n_e$(crit) | 8 | 2.36 | 0.168 | 0.19 | 0.029 | 0.92 | 0.999 |
| | FWZI vs. $\chi$ | 8 | 2.10 | 0.733 | 0.80 | 0.436 | 0.57 | 0.856 |

[a] The common logarithm (base 10) of each variable is used. Units are: width (km s$^{-1}$), density (cm$^{-3}$), $\chi$ (eV).

[b] Number of points (see Table 3). All points considered to be independent.

[c] Correlation coefficient.

[d] Probability that the two variables are correlated.

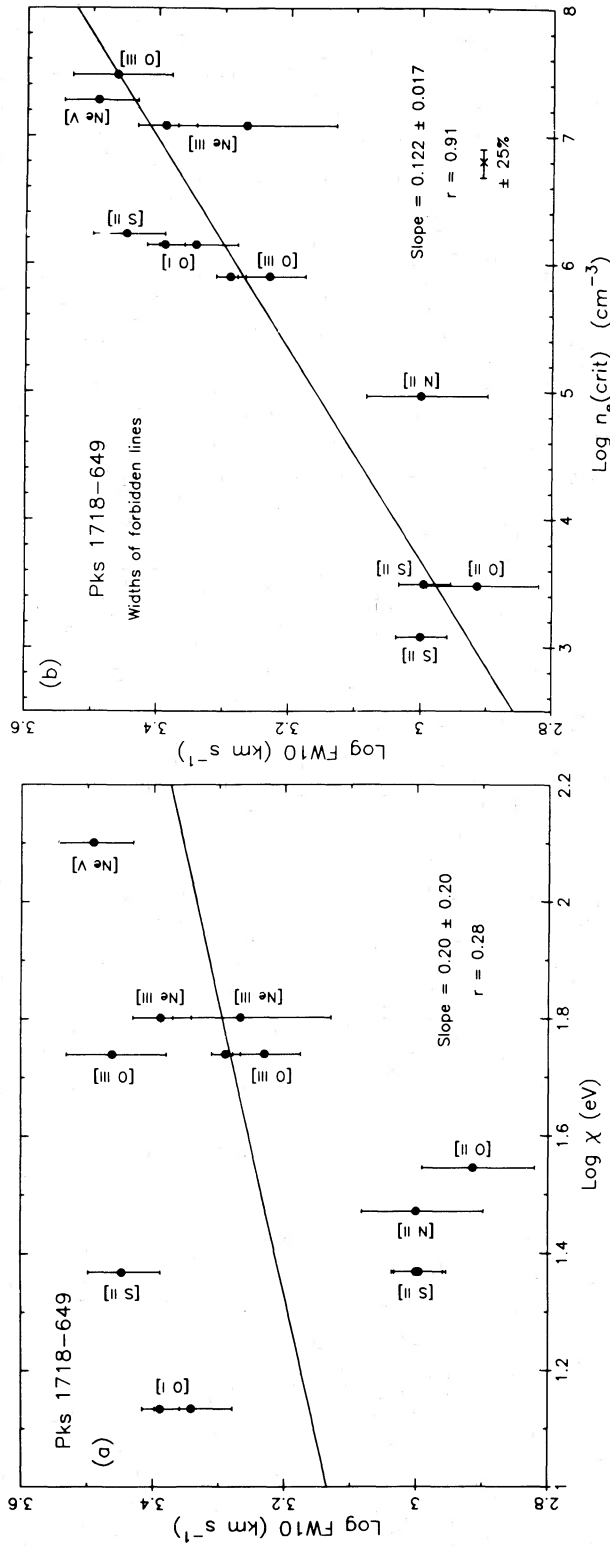[e] [Ne V] $\lambda3346$ excluded for consistency with FW10 (see Table 3).

Fig. 4.—(a) Log FW10 is plotted against Log χ for 13 forbidden lines in PKS 1718−649, where in each case χ is the ionization potential of the emitting species. The scatter is large: there is a 35% chance that the parent population is uncorrelated. If χ is replaced with $n_e$(crit) as in (b), the correlation coefficient increases from 0.28 to 0.91 and the probability of an uncorrelated parent population drops to virtually zero. An error bar of ±25% indicates probable uncertainties in theoretical calculations of $n_e$(crit).

observed Balmer decrement. After dereddening the lines by $A_v = 0.70$ mag (derived in § III$a$), Table 2 shows that $I(\mathrm{H}\alpha)/I(\mathrm{H}\beta)/I(\mathrm{H}\gamma)/I(\mathrm{H}\delta) = 3.64/1.00/0.47/0.26$, close to the theoretical decrement of $2.85/1.00/0.47/0.26$ (Brocklehurst 1971). Only $I(\mathrm{H}\alpha)/I(\mathrm{H}\beta)$ is discrepant, but the difference can be attributed to the broad component of H$\alpha$.

### IV. PICTOR A

Pictor A is a 16th mag elliptical galaxy at a distance of $\sim 210$ Mpc. Conspicuous optical emission lines (Schmidt 1965) and the object's association with a strong double-lobed radio source led to its classification as an N galaxy. Although the spectral index of the extended radio structure is $\sim 0.9$, Pictor A also exhibits a compact unresolved core having a flat or even inverted spectrum. Its infrared colors are consistent with a nonstellar continuum of power-law shape (Glass 1981), and it is a source of hard X-rays (Marshall *et al.* 1979). A bright, almost unresolved nucleus is visible in photographs of short exposure. The optical emission lines have both narrow and broad components (Danziger, Fosbury, and Penston 1977, hereafter DFP); in particular, the broad wings of H$\alpha$ have FWZI $\gtrsim 20,000$ km s$^{-1}$, and the profile of [O I] $\lambda 6300$ is much wider than those of [S II] $\lambda\lambda 6716, 6731$. This is very similar to NGC 7213, and inspired the detailed study discussed below.

#### a) Data

A new optical spectrum, convolved with a Gaussian having 5.3 Å FWHM to produce a resolution of $\sim 7$ Å, is presented in Figure 5. The object's redshift ($cz = 10,520$ km s$^{-1}$) was obtained by averaging the observed wavelengths of [O I], [S II], H$\alpha$, H$\beta$, and H$\gamma$. High-ionization lines ([O III] $\lambda\lambda 4959$, 5007, [Ne III] $\lambda 3869$) exhibit small relative blueshifts ($\sim 60$ km s$^{-1}$) like those in PKS 1718−649 and many other AGNs (e.g., Grandi 1978; Wilson 1979). Velocity widths, equivalent widths, and intensities of emission lines were carefully determined (Tables 2 and 3) with the techniques described in § III$b$ and by

FH. DFP only measured peak intensities in the central cores of lines, resulting in a number of discrepancies with the ratios in Table 2.

As in type 1 Seyferts and quasars, the continuum is nearly featureless; Ca II K has an EW of only $\sim 1$ Å, and that of the G band ($\lambda 4304$) is $\lesssim 1.5$ Å. The continuum is therefore predominantly nonstellar. High-ionization lines such as He II $\lambda 4686$, [Ne III], and [Fe VII] indicate that it continues blueward to energies of at least $\sim 100$ eV, photoionizing gas near the nucleus. H$\alpha$ emission is very broad (FWZI $\gtrsim 22,000$ km s$^{-1}$), with logarithmic wings to first order [$I(\Delta\lambda) \sim C_1 \mathrm{Log}(\Delta\lambda) + C_2$, where $C_1$ and $C_2$ are constants]. Comparison with the data of DFP shows that its intensity and profile vary with time. Broad emission is also visible in H$\beta$ and He II $\lambda 4686$, as emphasized by Figure 6; its great intensity in He II $\lambda 4686$ relative to H$\beta$ implies a high ionization parameter ($U \approx 0.01$) in the BLR (Halpern 1982). A component of intermediate width can be seen in the base of the [O III] $\lambda 5007$ profile by viewing Figure 6 at a glancing angle along the ordinate.

#### b) Analysis

Figure 1$b$ illustrates a quantitative decomposition of the optical continuum (as in § III$a$). The best fit is obtained when the data are dereddened by $A_v = 0.17$ mag, and a value of $\sim 1.1 \pm 0.5$ is derived for $\alpha$. Unlike the case in PKS 1718−649, the nonstellar component dominates starlight by a wide margin: at $\lambda 4000$, stars account for $\sim 9\%$ of the total flux, and even in the red their contribution is only $\sim 20\%$. Objects with a less prominent nonstellar component than in PKS 1718−649, or a stronger one than in Pictor A, would be difficult to illustrate in a manner analogous to that used here, so Figure 1 nicely represents two rather extreme cases.

Simple extrapolation of the power-law continuum to UV energies predicts an H$\alpha$ flux of $9.9 \times 10^{-14}$ ergs s$^{-1}$ cm$^{-2}$ if H$\alpha$ is produced entirely by recombination of photoionized gas and if the covering fraction ($F_c$) is unity. This is nearly a factor
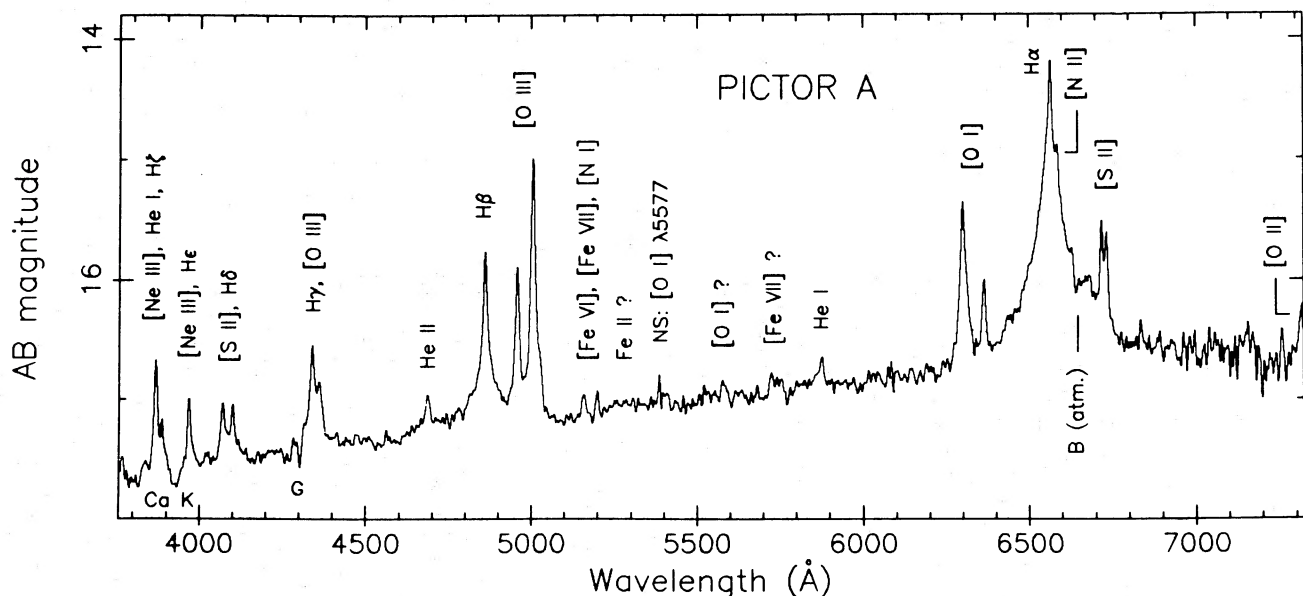


FIG. 5.—A dereddened ($A_v = 0.17$ mag) spectrum of the central $2'' \times 4''$ of Pictor A. As in all other spectra displayed in this paper, the systemic velocity was removed by replacing $\lambda$ with $\lambda/(1 + z)$ as well as $f_v$ with $f_v/(1 + z)$ in each bin; thus, the computed emission-line fluxes remain unchanged. The data were Gaussian-smoothed to a resolution of $\sim 7$ Å. Relative fluxes are accurate to $\sim 10\%$, except redward of $\sim \lambda 6200$ (see text). The absolute calibration is uncertain due to thin clouds and the small entrance aperture. NS refers to the poorly subtracted [O I] $\lambda 5577$ night sky line.
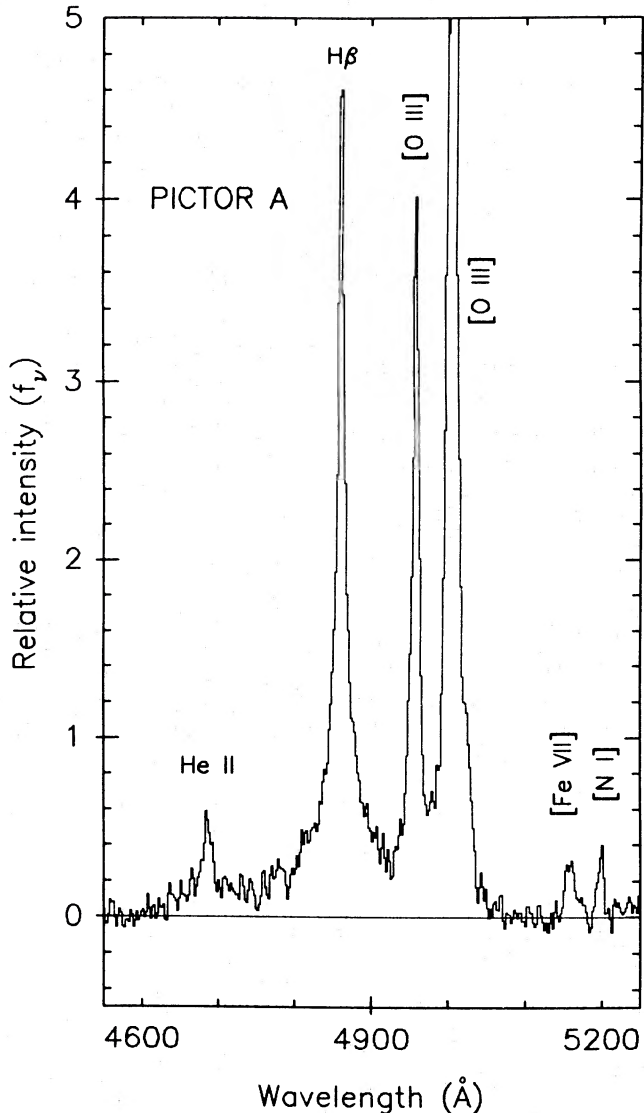
FIG. 6.—A portion of the Pictor A spectrum illustrates the wide range of ionization, including lines of [N I] and [Fe VII]. The intensity of He II $\lambda4686$ relative to H$\beta$ is much greater in the broad wings than in the narrow cores, indicating that the ionization parameter is higher in the broad-line region. Inspection of the spectrum at a glancing angle along the ordinate reveals a distinct red "shoulder" in the profile of [O III] $\lambda5007$.

prototypical shock-heated galaxy. In fact, comparison with the supernova remnant N49 (Osterbrock and Dufour 1973), the Cygnus Loop (Miller 1974), and the models of Cox (1972) led DFP to conclude that gas in Pictor A is heated by shocks. Their hypothesis was supported by the anomalously intense [O III] $\lambda4363$, from which they derived a temperature too high ($\sim 30,000$ K) to be compatible with photoionization. How, then, can all these properties be mutually consistent?

Casual inspection of Figure 3$b$ hints that the answer is exactly the same as for PKS 1718−649 and NGC 7213: [O I] $\lambda6300$ is much broader than each of the [S II] $\lambda\lambda6716$, 6731 lines, suggesting that clouds of different density and velocity exist in the NLR. Figures 7$a$ and 7$b$ provide compelling evidence for this, since line widths are once again much better correlated with $n_e$(crit) than with $\chi$ (FH; § III).

Relevant parameters of the unweighted, linear least-squares fits are given in Table 4. A correlation between line width and $\chi$ may be present, but this is to be expected even if $n_e$(crit) is the fundamental parameter because $\chi$ generally increases with increasing $n_e$(crit) for strong optical emission lines. Outstanding exceptions are [O I] $\lambda6300$ and [S II] $\lambda4069$, and it is precisely these lines (together with [O III] $\lambda4363$) that produce such a clear distinction between the two relations in Figure 7. It is interesting that corresponding points in Figures 4$b$ and 7$b$ have approximately the same positions relative to the line of best fit. The points representing [O III], [O I], and [S II] near Log [$n_e$(crit)] $\approx 6$ are good examples of this.

Under the assumption that each line is emitted by clouds whose density is equal to the appropriate value of $n_e$(crit), Table 4 shows that FWHM $\propto n^{0.103 \pm 0.015}$ in Pictor A. A larger slope is obtained if the FW10, rather than FWHM, is measured: FW10 $\propto n^{0.161 \pm 0.022}$. These findings agree well with the model of optically thick clouds in gravitational infall proposed by Carroll and Kwan (1983; see also Kwan and Carroll 1982), which explicitly predicts that width should increase with density. In this model, a low-density reservoir produces relatively strong, narrow cores in the emission lines and reduces the variation of FWHM relative to that of FWZI (or FW10). The low-density gas is not always significant, however, as evidenced by PKS 1718−649 and NGC 7213 (FH).

Comparable widths of [N II] $\lambda6583$ [$n_e$(crit) $\approx 9 \times 10^4$ cm$^{-3}$] and lines characterized by a much smaller $n_e$(crit) of $\sim 2 \times 10^3$ cm$^{-3}$ ([S II] $\lambda6724$, [O II] $\lambda3727$, [N I] $\lambda5200$) suggest that the latter lines are all emitted primarily from the low-density reservoir ($n_e \approx 10^3$ cm$^{-3}$), which does not participate in the gravitational infall (Carroll and Kwan 1983). [N II] $\lambda6583$, on the other hand, is probably produced mainly in clouds of considerably higher density. Linear fits to [N II] and the other high-density species (omitting those of low-density mentioned above) in the correlation between FWHM and $n_e$(crit) give somewhat steeper slopes than listed in Table 4; that of Pictor A is 0.15 rather than 0.10, while in PKS 1718−649 it is 0.17 (instead of 0.11). As discussed by FH, a slope of $\sim 0.25$ is expected if clouds move in Keplerian orbits while maintaining a constant ionization parameter, $U$.

Approximate constancy of $U$ is an important result of the two-phase model of QSO emission-line regions (Krolik, McKee, and Tarter 1981), in which cold clouds are confined by a hot intercloud medium, and a natural extension of this model to the NLR was possible in NGC 7213 (FH). It may also be applicable to Pictor A and PKS 1718−649 since they exhibit a similar correlation between line width and $n_e$(crit). The slopes

of 3 smaller than the observed (dereddened) intensity, and the discrepancy increases if $F_c < 1$. As in PKS 1718−649, a "UV bump" may account for the deficit; its presence is likely in view of the great similarity between Pictor A and other Seyfert 1 galaxies. Furthermore, the steep Balmer decrement suggests that some H$\alpha$ emission is due to collisional enhancement in the high-density clouds ($n \approx 10^9$ cm$^{-3}$) which inhabit the BLR (Kwan and Krolik 1981).

The featureless continuum, luminous X-ray source, and rich emission-line spectrum of Pictor A demonstrate that gas is undoubtedly photoionized by nonstellar radiation. On the other hand, the great intensity of [O II] $\lambda3727$ and especially [O I] $\lambda6300$ relative to [O III] $\lambda5007$ (DFP; Table 2) make Pictor A a "transition" object between Seyfert galaxies and Liners (Heckman 1980). The observed intensity ratios are reminiscent of those in NGC 1052, which is often regarded as the
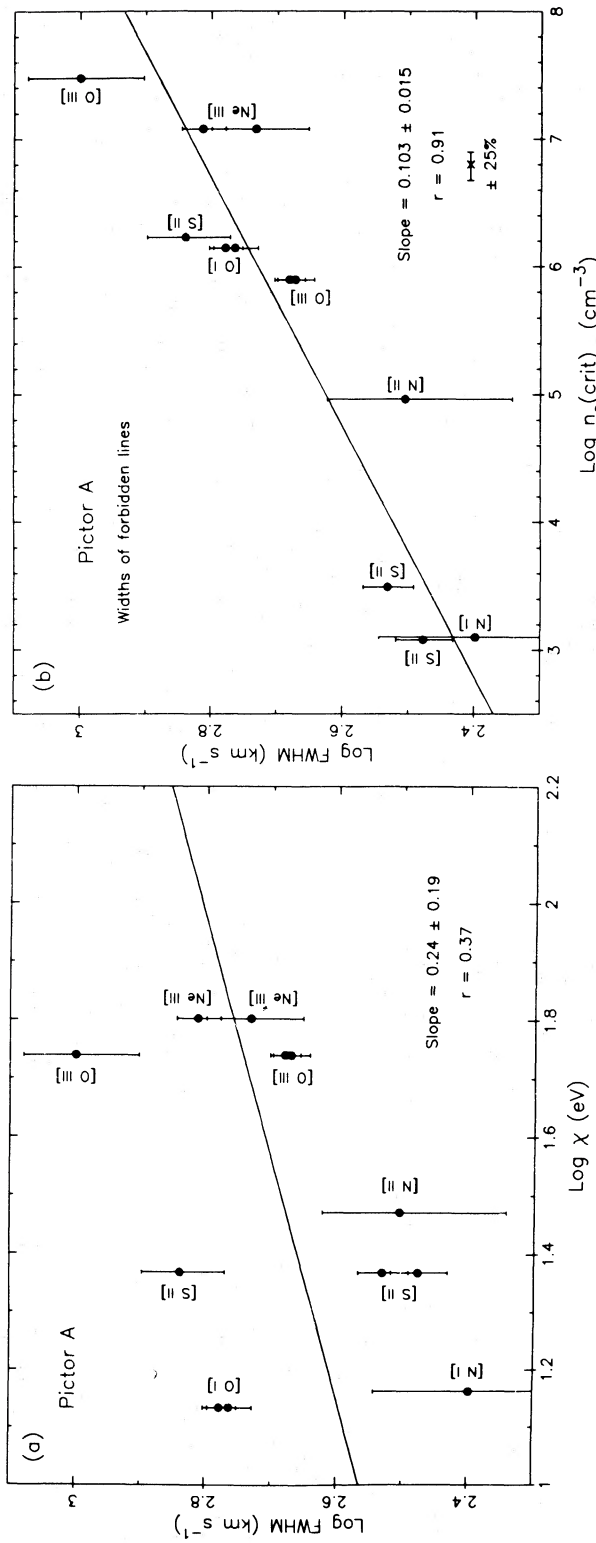
FIG. 7.—(a) The presence of a correlation (probability = 0.76) between line width and χ is marginal in Pictor A. Different lines from the same species (e.g., [S II]), however, have very disparate widths, suggesting that χ is not the fundamental parameter. As in PKS 1718−649, the correlation is greatly improved (b) if the appropriate critical density, rather than χ, is used for each forbidden line.

derived above, however, are significantly lower than required for constancy of $U$, so complete two-phase equilibrium is unlikely. Alternatively, the smaller slopes may simply indicate that the velocity of clouds decreases more slowly with increasing radial distance than in Keplerian orbits, a not unexpected result.

The [O III] ratio $R$, derived after careful subtraction of H$\gamma$ using the scaled profile of H$\beta$, is $\sim 14$. This is much smaller than the value obtained by DFP (who did not attempt to accurately deblend [O III] $\lambda 4363$ from H$\gamma$) and indicates $T_e \approx 5.6 \times 10^4$ K if $n_e \approx 10^4$ cm$^{-3}$. If the [S II] $\lambda\lambda 6716, 6731$ lines (intensity ratio $\approx 1.0$) are used to derive the density ($n_e \approx 450$ cm$^{-3}$), the temperature implied by $R$ is still higher. At a density of $\gtrsim 10^6$ cm$^{-3}$ in the O$^{++}$ zone, on the other hand (as suggested by Fig. 7$b$), $T_e \lesssim 15{,}000$ K and is consistent with photoionization models.

Pictor A thus exhibits a great range of densities, just as NGC 7213 and PKS 1718$-$649. Instead of the distinct narrow-line (low-density) and broad-line (high-density) regions often mentioned in connection with Seyfert 1 galaxies, a more or less continuous range is present. Values $\gtrsim 10^7$ cm$^{-3}$ are indicated by some forbidden lines (e.g., [O III] $\lambda 4363$), and the density must be still higher ($> 10^8$ cm$^{-3}$) in high-velocity clouds which produce the broad wings of permitted lines. Oddly enough, DFP saw "no evidence for the existence of a high-density component," even though their spectra clearly show wings in the [O I] profiles (compared with the nearby [S II] lines) and extremely broad Balmer emission.

### V. MR 2251$-$178

MR 2251$-$178 was the first QSO to be initially identified from X-ray observations (Ricker *et al.* 1978). Its optical flux varies on time scales of a few months, and a weak, unresolved radio source is present at $\sim 5$ GHz. Spectrophotometry by Canizares, McClintock, and Ricker (1978) revealed a strong emission-line spectrum ($cz \approx 0.0638$) dominated by broad permitted lines (FWZI $\approx 20{,}000$ km s$^{-1}$). Phillips (1980) showed that MR 2251$-$178 is associated with a cluster of $\sim 50$ galaxies, and that faint nebulosity surrounds the unresolved core. Detailed spectrophotometry by Bergeron *et al.* (1983, hereafter BBDT) demonstrated the additional presence of a giant

envelope of photoionized gas around the QSO and its parent galaxy.

Independent measurements indicate that the [O III] ratio $R$ is between 7 and 9 in the nucleus of MR 2251$-$178 (Canizares, McClintock, and Ricker 1978; BBDT), substantially lower than the normal value ($\sim 25$–50) for photoionized gas in AGNs. This is exactly the problem encountered in photoionization models of Liners. Furthermore, BBDT's spectrum shows two relatively distinct components in some of the forbidden lines, suggesting once again that clouds of different density exist in the NLR. New data were therefore obtained to investigate this possibility.

#### a) Data

The spectrum, obtained through an $8'' \times 8''$ aperture under photometric conditions, is illustrated in Figure 8. Only [O III] $\lambda 5007$ was noticeably affected by coincidence losses ($\sim 8\%$), although small inaccuracies may also exist in some of the other very strong emission lines. The instrumental resolution was $\sim 5.4$ Å, but the data in Figure 8 were smoothed with a Gaussian to yield a final value of $\sim 7$ Å. The spectrum was dereddened under the assumption of a normal reddening law and a Galactic $A_v$ of 0.05 mag (Burstein and Heiles 1982). A redshift of $0.06397 \pm 0.00005$ was calculated from the emission lines and removed. No systematic differences in redshift between high- and low-ionization lines were evident to within $\sim \pm 15$ km s$^{-1}$.

H$\beta$ has a FWZI of $\sim 25{,}000$–30,000 km s$^{-1}$ (depending on the adopted contribution of broad He II $\lambda 4686$). This means gas travels with $v \approx 0.04c$, and implies $M \gtrsim 10^9\ M_\odot$ for the central object *if* clouds at typical distances of $\sim 0.1$ pc move predominantly under its gravitational influence. For comparison, the total mass of clouds in the BLR is $\sim 100\ M_\odot$, calculated under the assumptions that $n_e \approx 10^9$ cm$^{-3}$ and that Balmer emission is produced entirely by recombination of ionized hydrogen.

Starlight is almost completely absent. The only measureable absorption feature is Ca II K, whose equivalent width ($\sim 0.2$ Å) demonstrates that stars contribute $\lesssim 2\%$ of the flux near $\lambda 4000$. Since a large aperture was used, the strength of the line is increased by the galactic nebulosity surrounding the QSO itself; the ratio of nonstellar to stellar flux in the unresolved nucleus is $\gtrsim 100$. Complementing the featureless continuum is a prominent UV excess.
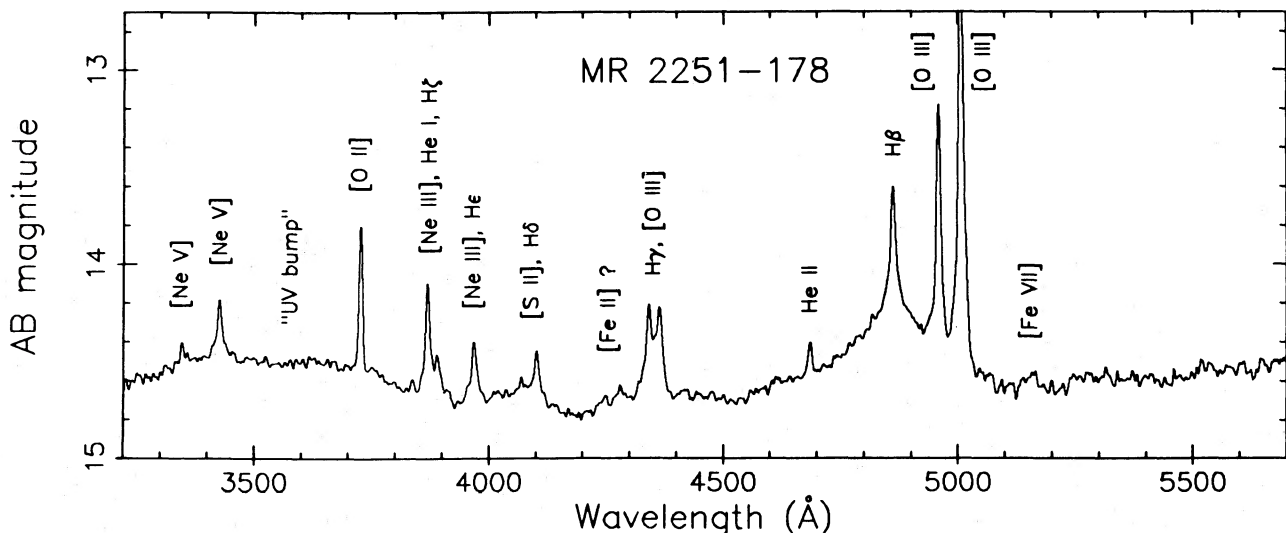


FIG. 8.—The spectrum of MR 2251$-$178, obtained under photometric conditions. A Galactic $A_v$ of 0.05 mag was used to deredden the data, which were smoothed with a Gaussian to produce a resolution of $\sim 7$ Å. The Balmer lines are very broad, and a prominent UV excess is visible.

### b) Analysis

Properties of emission lines were measured in the usual manner (Tables 2 and 3). Agreement with the results of BBDT is generally satisfactory, except for the weakest features and badly blended lines. A distinct, broad component of He II λ4686 is probably present but cannot be deblended from Hβ. The Balmer decrement is steeper than reported by BBDT, and the Balmer lines themselves are weaker relative to [O III] λ5007 and to the continuum. The equivalent width of Hβ is ~150 Å, compared with the published (BBDT) value of ~240 Å; this supports previous claims of optical variability in MR 2251−178.

As suspected, the forbidden lines display a range of profiles (Fig. 9). The [O II] λ3727 blend is narrow and does not exhibit appreciable wings. [O III] λ5007 (averaged with [O III] λ4959 in Fig. 9b), on the other hand, has significant extensions to the
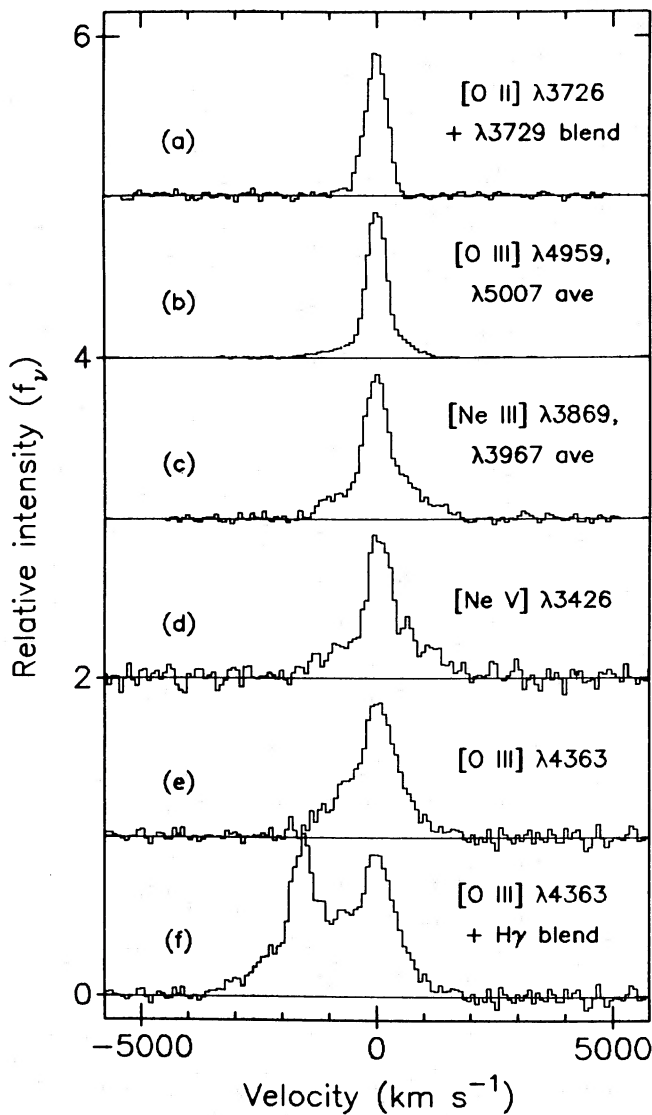


FIG. 9.—Profiles of five different emission lines, given in order of increasing $n_e$(crit), illustrate the presence of a range of densities in the NLR of MR 2251−178. The width and relative prominence of the broad base rises with $n_e$(crit). Marked differences are visible in lines arising from the same species, [O III], despite uncertainties in the deblending of [O III] λ4363 from Hγ (Figs. 9e and 9f).

blue and red. The strength of the broad component relative to the narrow core is still larger in the [Ne III] and [Ne V] lines. Finally, [O III] λ4363 is broader than [O III] λ5007, demonstrating that $n_e$(crit) (rather than χ) is once again the fundamental parameter. De Robertis and Osterbrock (1984) found that such a difference in the [O III] widths is a very general property of high-ionization Seyfert 1 galaxies.

Note that the deblending of [O III] λ4363 from Hγ (Figs. 9e and 9f) is uncertain, since Hγ was assumed to have a symmetrical core. A scaled version of Hβ could not be used to approximate Hγ because marked differences in unblended portions of the two profiles reveal that the Balmer decrement varies with velocity. The derived [O III] ratio R is ~10, somewhat higher than the estimates of BBDT and Canizares, McClintock, and Ricker (1978).

Figure 10 displays R as a function of velocity in the line profiles. Defining the peaks of the emission lines as zero, it is obvious that the strength of [O III] λ4363 relative to [O III] λ5007 increases dramatically in the broad wings. Under the simplifying assumption of constant temperature ($T_e = 15,000$ K) in the photoionized gas, this means that the density in clouds increases monotonically with their velocity. Higher densities ($\gtrsim 5 \times 10^6$ cm$^{-3}$) probably occur at even greater velocities than could be shown in Figure 10 (due to the limited S/N ratios); similarly, the lowest densities (~$10^6$ cm$^{-3}$) represent only an upper limit because of contamination from dense, high-velocity clouds moving transversely to the line of sight. The increase of cloud velocity with density is confirmed by the strong correlation between width and $n_e$(crit) for lines produced by different species (Table 4). Thus, MR 2251−178 exhibits the same behavior as PKS 1718−649 and Pictor A in this respect.

### VI. DISCUSSION AND CONCLUSIONS

Recent investigations show that the spectral characteristics of Liners can be explained in the context of Seyfert photoionization models. A well-known difficulty, however, is that $T_e$ remains constrained to $\lesssim 20,000$ K while in many Liners the great strength of [O III] λ4363 implies temperatures exceeding 30,000 K. High $T_e$ in the O$^{++}$ zone, on the other hand, is a natural consequence of shock heating (e.g., Shull and McKee 1979).

Here the problem is resolved in at least one Liner by the discovery of a great range of densities among the clouds of gas. Densities between 200–300 cm$^{-3}$ and ~$10^6$–$10^7$ cm$^{-3}$ must exist in PKS 1718−649, as shown by the $I$([S II] λ6716)/$I$([S II] λ6731) ratio together with the observed correlation between line width and $n_e$(crit). This is much larger than the range reported in most type 2 Seyferts (Koski 1978), but it has sometimes been deduced from measurements of the [O III] and [Ar IV] lines in broad-line radio galaxies (Osterbrock, Koski, and Phillips 1976), type 1 Seyferts (Neugebauer et al. 1976; Osterbrock 1977), and quasars (e.g., Baldwin 1975). Filippenko and Sargent (1985) argue that such conditions are probably also common in classical Liners, as [O I] λ6300 [$n_e$(crit) $\approx$ 1.4 × 10$^6$ cm$^{-3}$] is often considerably broader than each of the [S II] λλ6716, 6731 lines [$n_e$(crit) $\approx$ 2 × 10$^3$ cm$^{-3}$]. Moreover, they show that at least one-third of all Liners exhibit a weak, broad component of Hα similar to (but much fainter than) that produced by the high-density BLR in QSOs and Seyfert 1 galaxies. Previous workers had neglected the possibility of high densities in Liners, since most spectra had not been of sufficient quality to reveal the different line widths.
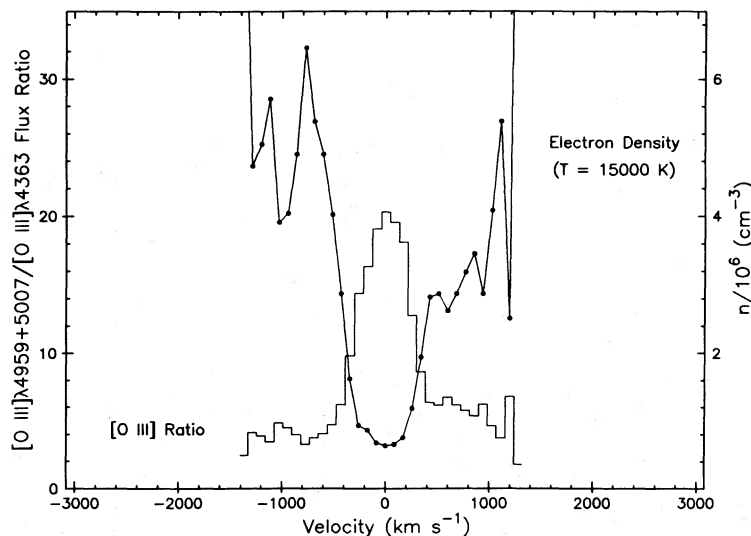
FIG. 10.—The ratio $I([O\ III]\ \lambda\lambda4959+5007)/I([O\ III]\ \lambda4363)$ is plotted against velocity (i.e., position in the line profile) for MR 2251−178. The zero-point corresponds to the peak of each line. Using $T_e = 15,000$ K, the derived value of $n_e$ is also given. The ordinate scale at left refers to the [O III] flux ratio; that at right, to the density. Low-velocity clouds are clearly the least dense, especially if contamination of the emission-line cores by high-density clouds moving transversely to the line of sight is taken into account.

Dense gas contributes strongly to auroral and transauroral lines, thereby mimicking the effects of high $T_e$. The actual temperature, however, can easily be compatible with photoionization models, so shocks need not be invoked. This is clearly illustrated by spectra of the QSO MR 2251−178 and the Seyfert/Liner galaxy Pictor A—lines in these objects are *undoubtedly* produced by photoionized gas, yet they too exhibit the "high $T_e$" problem discussed above *unless* the dense NLR clouds revealed by the different line widths are taken into account. The same can be said for NGC 7213 (FH) and probably even PKS 1718−649, except the relative intensities of their ionizing continua are not as great.

Although neither Pictor A nor NGC 7213 can be considered "typical" Liners because of their obvious features of Seyfert 1 galaxies, they provide a crucial link between the two classes. It is important to notice that Heckman's (1980) original definition of a Liner (in terms of [O I], [O II], and [O III] line strengths) contains no reference to the presence or absence of a nonstellar continuum, broad Hα, or other properties generally associated with classical AGNs. Hence, a type 1 Seyfert galaxy may also have characteristics which place it near the Liner domain, as is the case with Pictor A and NGC 7213.

The correlation between line width and $n_e$(crit) in all four galaxies studied here and by FH suggests that clouds move through the NLR in very roughly Keplerian orbits. Detailed models based on this idea (Kwan and Carroll 1982; Carroll and Kwan 1983) show that most of the emission is produced by clouds falling toward the nucleus. The densities, line widths, and some important relative intensities are in excellent quantitative agreement with the new results. The densest clouds are optically thick to the Lyman continuum, so that every ionization stage (up to a certain level) is included in each cloud. Strong [O I] is produced in a vast region of partially ionized (∼10%) hydrogen (Halpern 1982).

A model developed by Péquignot (1984) concentrates on emission-line intensity ratios in greater detail. Péquignot concludes that the spectral characteristics of NGC 1052 (and perhaps of other Liners as well) *require* a density stratification of the type reported here; single-density models fall far short of

providing adequate agreement. Moreover, he suggests that the observed He II $\lambda4686$ emission is weaker than that predicted by simple power-law photoionization models because the *actual* ionizing radiation is primarily that of a hot blackbody ($T \approx 8 \times 10^4$ K) prolonged by a flat, soft X-ray continuum. Since the thermal spectrum has a pronounced maximum between 13.6 and 54.5 eV, very little He II $\lambda4686$ is produced in comparison with the Balmer lines. This is consistent with galaxies such as NGC 7213 (Fig. 2 in FH) and PKS 1718−649 (Fig. 2), in which no He II $\lambda4686$ at all is visible prior to the removal of an absorption-line template.

Some difficulties with photoionization models still remain, but these do not seem fundamental or insurmountable. The predicted strength of [N I] $\lambda5200$, for example, is too large in almost all models (e.g., Halpern 1982; Ferland and Netzer 1983). This may partly be resolved by adopting a higher minimum density in the clouds, since $n_e$(crit) is very small (Péquignot 1984). Furthermore, the abundance of N° may be affected by physical processes (such as ionization from an excited level of N$^+$) which are not fully treated by at least some models (Halpern 1984).

In summary, these data demonstrate that a variety of AGNs have narrow-line clouds which span a great range in density and velocity. Virtually the same conclusions were drawn in the analysis of a classical Liner (PKS 1718−649), two "transition" galaxies between Liners and Seyferts (NGC 7213, Pictor A), and a nearby QSO (MR 2251−178). The respective flux of Hβ from the nuclei of these objects is very roughly 3, 5, 30, and 1600 in units of $10^{40}$ ergs s$^{-1}$, and the intensity of a blue nonstellar continuum follows a comparable progression. Since Balmer emission and nonstellar radiation are indicators of "activity" in galactic nuclei, the results suggest that physical conditions and processes are similar in all these objects.

Specifically, they imply that photoionization, rather than shock heating, is the dominant excitation mechanism even in Liners. To test this, a sensitive search for weak nonstellar continua, [Ne V] $\lambda3426$, broad Hα emission, and correlations between line width and critical density must be made in large numbers of Liners. Some initial surveys have already been con-

ducted (Stauffer 1982; Keel 1983), and much more detailed ones are in progress (Filippenko and Sargent 1985). Preliminary results indicate the presence of these features in many objects, as well as substantial continuity in their prominence, and therefore provide strong support for the photoionization hypothesis.

*Note added in manuscript, 1984 October 12.*—After this work was completed, I received a paper by Carswell *et al.* (1984) on PKS 1718−649 and Pictor A. The main results of these authors are consistent with mine, although their data and analysis are not as extensive. In particular, Carswell *et al.* (1984) are unable to conclude with confidence that PKS 1718−649 is photoionized because they do not detect He II $\lambda4686$, [Ne v] $\lambda3426$, broad H$\alpha$ emission, and the nonstellar continuum. Moreover, the $S/N$ ratios in their spectra are not sufficiently high to unambiguously demonstrate a correlation between width and $n_e$(crit) for a large number of lines in Pictor A and PKS 1718−649. From an analysis of a few species (e.g., [O I], [O III]), however, they correctly deduce that high densities must be present in the NLR of each object, and that the gas is probably stratified.

## REFERENCES

Baldwin, J. A. 1975, *Ap. J.*, **201**, 26.
Baldwin, J. A., Phillips, M. M., and Terlevich, R. 1981, *Pub. A.S.P.*, **93**, 5.
Bergeron, J., Boksenberg, A., Dennefeld, M., and Tarenghi, M. 1983, *M.N.R.A.S.*, **202**, 125 (BBDT).
Brocklehurst, M. 1971, *M.N.R.A.S.*, **153**, 471.
Burstein, D., and Heiles, C. 1982, *A.J.*, **87**, 1165.
Butler, S. E., Heil, T. G., and Dalgarno, A. 1980, *Ap. J.*, **241**, 442.
Canizares, C. R., McClintock, J. E., and Ricker, G. R. 1978, *Ap. J. (Letters)*, **226**, L1.
Carroll, T. J., and Kwan, J. 1983, *Ap. J.*, **274**, 113.
Carswell, R. F., Baldwin, J. A., Atwood, B., and Phillips, M. M. 1984, *Ap. J.*, **286**, 464.
Cox, D. P. 1972, *Ap. J.*, **178**, 143.
Danziger, I. J., Fosbury, R. A. E., and Penston, M. V. 1977, *M.N.R.A.S.*, **179**, 41P (DEP).
Davidson, K., and Netzer, H. 1979, *Rev. Mod. Phys.*, **51**, 715.
De Robertis, M. M., and Osterbrock, D. E. 1984, *Ap. J.*, **286**, 171.
Elvis, M., Soltan, A., and Keel, W. C. 1984, *Ap. J.*, **283**, 479.
Ferland, G. J. 1981, *Ap. J.*, **249**, 17.
Ferland, G. J., and Netzer, H. 1983, *Ap. J.*, **264**, 105.
Filippenko, A. V. 1982, *Pub. A.S.P.*, **94**, 715.
———. 1985, in preparation.
Filippenko, A. V., and Greenstein, J. L. 1984, *Pub. A.S.P.*, **96**, 530.
Filippenko, A. V., and Halpern, J. P. 1984, *Ap. J.*, **285**, 458 (FH).
Filippenko, A. V., and Sargent, W. L. W. 1985, *Ap. J. Suppl.*, in press.
Fosbury, R. A. E., Mebold, U., Goss, W. M., and Dopita, M. A. 1978, *M.N.R.A.S.*, **183**, 549.
Fosbury, R. A. E., Mebold, U., Goss, W. M., and van Woerden, H. 1977, *M.N.R.A.S.*, **179**, 89 (FWGV).
Glass, I. S. 1981, *M.N.R.A.S.*, **197**, 1067.
Grandi, S. A. 1978, *Ap. J.*, **221**, 501.
Gunn, J. E. 1979, in *Active Galactic Nuclei*, ed. C. Hazard and S. Mitton (Cambridge: Cambridge University Press), p. 213.
Halpern, J. P. 1982, Ph.D. thesis, Harvard University.
———. 1984, private communication.
Halpern, J. P., and Filippenko, A. V. 1984, *Ap. J.*, **285**, 475.
Halpern, J. P., and Steiner, J. E. 1983, *Ap. J. (Letters)*, **269**, L37.
Heckman, T. M. 1980, *Astr. Ap.*, **87**, 152.
Keel, W. C. 1983, *Ap. J.*, **269**, 466.

Keel, W. C., and Miller, J. S. 1983, *Ap. J. (Letters)*, **266**, L89.
Koski, A. T. 1978, *Ap. J.*, **223**, 56.
Koski, A. T., and Osterbrock, D. E. 1976, *Ap. J. (Letters)*, **203**, L49.
Krolik, J. H., McKee, C. F., and Tarter, C. B. 1981, *Ap. J.*, **249**, 422.
Kwan, J., and Carroll, T. J. 1982, *Ap. J.*, **261**, 25.
Kwan, J., and Krolik, J. H. 1981, *Ap. J.*, **250**, 478.
Lawrence, A., and Elvis, M. 1982, *Ap. J.*, **256**, 410.
Malkan, M. A., and Filippenko, A. V. 1983, *Ap. J.*, **275**, 477.
Malkan, M. A., and Sargent, W. L. W. 1982, *Ap. J.*, **254**, 22.
Marshall, F. E., Boldt, E. A., Holt, S. S., Mushotzky, R. F., Pravdo, S. H., Rothschild, R. E., and Serlemitsos, P. J. 1979, *Ap. J. Suppl.*, **40**, 657.
Miller, J. S. 1974, *Ap. J.*, **189**, 239.
Neugebauer, G., Becklin, E. E., Oke, J. B., and Searle, L. 1976, *Ap. J.*, **205**, 29.
Oke, J. B. 1978, *J.R.A.S. Canada*, **72**, 121.
Oke, J. B., Shields, G. A., and Korycansky, D. G. 1984, *Ap. J.*, **277**, 64.
Osterbrock, D. E. 1977, *Ap. J.*, **215**, 733.
Osterbrock, D. E., and Dufour, R. J. 1973, *Ap. J.*, **185**, 441.
Osterbrock, D. E., Koski, A. T., and Phillips, M. M. 1976, *Ap. J.*, **206**, 898.
Pelat, D., Alloin, D., and Fosbury, R. A. E. 1981, *M.N.R.A.S.*, **195**, 787.
Péquignot, D. 1984, *Astr. Ap.*, **131**, 159.
Piccinotti, G., Mushotzky, R. F., Boldt, E. A., Holt, S. S., Marshall, F. E., Serlemitsos, P. J., and Shafer, R. A. 1982, *Ap. J.*, **253**, 485.
Phillips, M. M. 1980, *Ap. J. (Letters)*, **236**, L45.
Ricker, G. R., Clarke, G. W., Doxsey, R. E., Dower, R. G., Jernigan, J. G., Delvaille, J. P., MacAlpine, G. M., and Hjellming, R. M. 1978, *Nature*, **271**, 35.
Rose, J. A., and Tripicco, M. J. 1984, *Ap. J.*, **285**, 55.
Savage, A. 1976, *M.N.R.A.S.*, **174**, 259.
Schmidt, M. 1965, *Ap. J.*, **141**, 1.
Shectman, S. A. 1981, in *Ann. Rept. Dir. Mt. Wilson and Las Campanas Observatories* (Washington: Carnegie Institution of Washington), p. 586.
Shectman, S. A., and Hiltner, W. A. 1976, *Pub. A.S.P.*, **88**, 960.
Shuder, J. M. 1981, *Ap. J.*, **244**, 12.
Shull, J. M., and McKee, C. F. 1979, *Ap. J.*, **227**, 131.
Stauffer, J. R. 1982, *Ap. J.*, **262**, 66.
Ulrich, M.-H., and Péquignot, D. 1980, *Ap. J.*, **238**, 45.
Wilson, A. S. 1979, *Proc. Roy. Soc. London, A*, **366**, 461.
Whitford, A. E. 1958, *A.J.*, **63**, 201.
Yee, H. K. C., and Oke, J. B. 1978, *Ap. J.*, **226**, 753.

ALEXEI V. FILIPPENKO: Department of Astronomy, University of California, Berkeley, CA　94720